

Single/multi-objective inverse robust evolutionary design methodology in the presence of uncertainty

Dudy Lim, Yew-Soon Ong, Meng-Hiot Lim, Yaochu Jin

2007

Preprint:

This is an accepted article published in Evolutionary Computation in Dynamic and Uncertain Environments. The final authenticated version is available online at: [https://doi.org/\[DOI not available\]](https://doi.org/[DOI not available])

Single/Multi-objective Inverse Robust Evolutionary Design Methodology in the Presence of Uncertainty: *Nominal, Robustness and Opportunity*

Dudy Lim¹, Yew-Soon Ong¹, Meng-Hiot Lim² and Yaochu Jin³

¹School of Computer Engineering, Nanyang Technological University
Nanyang Avenue, Singapore 639798
{dlim, asysong}@ntu.edu.sg

²School of Electrical and Electronics Engineering, Nanyang Technological University
Nanyang Avenue, Singapore 639798
EMHLIM@ntu.edu.sg

³Honda Research Institute Europe GmbH
Carl-Legien-Strasse 30, 63073 Offenbach
Yaochu.Jin@honda-ri.de

Abstract. Many existing works for handling uncertainty in problem-solving rely on some form of *a priori* knowledge of the uncertainty structure. However, in reality, one may not always possess the necessary expertise or sufficient knowledge to identify suitable bounds of the uncertainty involved. Rather, it is more likely that specifications of the realistic performance desired are derived, which may be based on the maximum degradation tolerable or worst-case performance permissible in the final solution. In this paper, we present a Single/Multi-objective Inverse Robust Evolutionary (SMIRE) optimization methodology. In contrast to conventional forward robust optimization, an inverse approach based on non-probabilistic methods is introduced to avoid making possible erroneous assumptions about the uncertainty when insufficient field data exists for accurately estimating its structure. Further, since uncertainty is practically impossible to avoid, we consider the possible benefits as the uncertainty prevails by introducing an *opportunity criterion* in the inverse search scheme. Four inverse schemes are presented to include the different objectives possibly considered in robust evolutionary optimization. The inverse schemes are applied on synthetic test functions to illustrate their utility.

1 Introduction

Evolutionary Algorithm (EA) [1] is a modern stochastic optimization technique that has emerged as a prominent contender for global optimization in complex engineering problem-solving. Its popularity lies in the ease of implementation and the ability to arrive close to the global optimum solution with reasonable computational budget. Most early studies in the literature on the application of EAs to complex engineering design have mainly emphasized on locating the global optimal design using determi-

nistic computational models. However, in many real-world problems, uncertainties are often present and practically impossible to avoid. In the case where a solution is very sensitive to small variations either in the system's variables or the operating conditions, it may not be desirable to put it into practice. Hence optimization without taking uncertainty into consideration generally leads to solutions that should not be labeled as optimal as they are likely to perform differently when put into practice.

Various classifications of uncertainty have been suggested over the recent years [2-8]. In [2], four types of uncertainty were described. They are 1) noise at fitness function, 2) uncertainty at design variables or environmental parameters, 3) approximation errors, and 4) time varying fitness function. Similar categorization can also be found in [3]. Others [4-5] classify uncertainty as either *aleatory* or *epistemic*. Aleatory uncertainty refers to naturally irreducible variability, e.g. quantities that are inherently variable over time and space. In contrast, epistemic uncertainty is caused by incomplete knowledge about the designs to be optimized and should be reducible if greater knowledge can be acquired. In [6-8], uncertainty is defined as the gap between the known and unknown facts. In this paper, we follow the categorization of uncertainty in [2] and [3]. In particular, we focus on uncertainty in the system's variables and/or environmental parameters.

To date, many approaches exist for coping with uncertainty in complex engineering design optimization. These include the One-at-a-Time Experiments, Taguchi Orthogonal Arrays, bounds-based, fuzzy and probabilistic methods [9]. In the context of EA, a number of prominent new studies on handling the presence of uncertainty in engineering designs have emerged recently. In [10], a Genetic Algorithm with Robust Searching Scheme (GA/RS3) was introduced. In this work, a probabilistic noise vector is added to the genotype before fitness evaluation. In biological terms, this means that part of the phenotypic features of an individual is determined by the decoding process of the genotypic code of genes in the chromosomes. The study of an (1+1)-Evolutionary Strategy (ES) with isotropic normal mutations using the noisy phenotype scheme has also been reported in [11]. An evolutionary algorithm based on max-min optimization strategy using a Baldwinian trust-region framework that employs surrogate models was also recently proposed in [3] for robust design. Recent applications of these robust EA strategies to engineering design problems include 2D aerodynamic airfoil [3,12], lightweight space structures [13] and multilayer optical coating design [14].

In this paper, we present a Single/Multi-objective Inverse Robust Evolutionary (SMIRE) design search methodology. In contrast to conventional forward robust optimization, the inverse approach avoids making assumptions about the uncertainty structure in the formulation of the optimization search process. Making assumptions about the uncertainty that are not backed up by strong evidence in evolutionary design optimization can possibly lead to erroneous designs that could have catastrophic consequences. Further, most existing schemes for handling uncertainty in evolutionary design optimization have focused on probabilistic methods [10-14]. Since probability theory may be inappropriate when insufficient field data exists for accurately estimating the structure of the uncertainty, we consider non-probabilistic methods, particularly, convex modeling, in the SMIRE. We begin with a single objective IRE approach in search for robust designs that are resilient to maximum uncertainty, given

the worst-case performance permissible by the designers. Further, since uncertainty is practically impossible to avoid, we consider the possible benefits as the uncertainty prevails by introducing an *opportunity criterion* in the design search. To provide a trade-off between nominal, robustness, and/or opportunity in the final design solution, various multi-objective IRE schemes are introduced.

A motivating application for the proposed methodology perhaps is in the area of finance where portfolio design relies on the estimation of the expected returns on securities invested. The estimation is usually based on historical valuations of the securities and the deviation from the expected return on investment is crudely quantified as the risk level. One underlying assumption is that for longer investment horizon, the estimated return based on historical valuations is a good approximation of future returns. Such an investment planning scenario originated from Markovitz's pioneering work on portfolio optimization [15] and is usually hard to put into practice. One reason is that the uncertainty in estimation of the expected returns as mentioned. Although it appears that taking a very long term perspective on a portfolio may circumvent this source of uncertainty, it is seldom adhered to for practical reasons. Furthermore, with the current advance information technology and the dynamically changing macro-economics landscape, a "sit-and-wait" attitude towards a portfolio is no longer viable. To the best of our knowledge, there has not been any work the attempts to apply evolutionary algorithms based on an inverse optimization approach to portfolio structuring. based on an inverse optimization approach.

The rest of this paper is organized as follows. In Section 2, we provide a brief overview of robust evolutionary design optimization. Four inverse schemes for evolutionary design search in the presence of uncertainty are presented in Section 3. To illustrate their applications, section 4 provides an empirical study on a series of test functions with different complexities. Finally Section 5 concludes this paper.

2 Evolutionary Optimization in the Presence of Uncertainty

This section presents a brief overview on the fundamental aspects of evolutionary design in the presence of uncertainties. *Forward* optimization refers to those schemes where an optimal solution is sought based on some prior knowledge about the structure of the uncertainty. *Inverse* optimization, on the other hand, locates the target solution that satisfies some criteria specified by the designers. Here, we consider the general bound constrained nonlinear programming problem of the forms:

Forward Optimization:

$$\begin{aligned} \mathbf{Optimize} : & f(x) \\ \mathbf{Subject\ to} : & x_l \leq x \leq x_u \end{aligned} \quad (1)$$

or

Inverse Optimization:

$$\mathbf{Optimize} : f(x) - T \quad (2)$$

Subject to: $x_l \leq x \leq x_u$

where $f(x)$ is a scalar-valued objective function, T is the targeted output performance, $x \in \mathfrak{R}^d$ is the vector of design variables or environmental parameters, while x_l and x_u are vectors of lower and upper bounds for x .

Here, our focus is on EAs for robust engineering design optimization under uncertainties that arise in:

- i) design vector x

$$F(x) = f(x + \delta) \quad (3)$$

where $\delta = (\delta_1, \delta_2, \dots, \delta_k)$, is the noise in the design vector and $F(x)$ is the effective fitness of design vector x .

- ii) operating/environmental conditions

$$F(x) = f(x, c + \xi) \quad (4)$$

where $c = (c_1, c_2, \dots, c_n)$, is the nominal value of the environmental parameters and ξ is a random vector used to model variability in the operating conditions. Since both forms of uncertainty may be treated equivalently, we do not differentiate uncertainty in design variables and the operating conditions. In the rest of this paper, we refer both the uncertain design variables and environmental parameters as uncertain parameters for the sake of brevity.

2.1 Probabilistic and Non-Probabilistic Schemes

Evolutionary techniques for handling uncertainty based on probabilistic schemes usually assume prior knowledge about the structure of the uncertainty. For example, the uncertainties, δ and/or ξ , are often assumed to be Gaussian (normal), Cauchy, or uniformly distributed. Very often, a Gaussian distribution with zero mean and variance σ^2 , $N(0, \sigma^2)$ is considered for the uncertainty, by virtue of the central limit theorem. Consequently, the effective fitness function $F(x)$ for forward and inverse optimization can then be described as:

Forward probabilistic optimization:

$$F(x) = \int_{-\infty}^{\infty} f(x + \delta) \Phi(\delta) d\delta \quad (5)$$

or

Inverse probabilistic optimization:

$$F(x) = \int_{-\infty}^{\infty} (f(x+\delta) - T) \Phi(\delta) d\delta \quad (6)$$

where $\Phi(\delta)$ is the probability distribution of δ .

On the other hand, it is often the case in many real world engineering design problems that very little knowledge about the structure of the uncertainty involved is available. Making assumptions about the uncertainty that are not backed up by strong evidence in evolutionary design optimization can possibly lead to erroneous designs that could have catastrophic consequences. Instead of focusing on making any probably unjustifiable mathematical model out of the uncertainty, non-probabilistic methods may be used. Non-probabilistic approaches have attracted increasing attention in the engineering design community in recent years. They include evidence theory, possibility theory, interval analysis, and convex modeling. For example, interval analysis and convex modelling studies the uncertain parameters x for some intervals $[x_l, x_u]$, where x_l and x_u are the lower and upper bound and how this range affects the design solutions. Nevertheless, while non-probabilistic approaches generally require minimum assumption about the uncertainty involved, they can incur a high computational cost [3, 16]. For the details of non-probabilistic approaches in design optimization, the reader is referred to [3, 6, 16].

2.2 Benefits of Uncertainty

In most design optimization schemes, uncertainty has always been viewed upon as harmful to the final design solution. More specifically, the performance of the final design is believed to deteriorate in practice as the result of uncertainty. Since uncertainties are practically impossible to avoid, it is worth asking whether possible benefits can be derived from the presence of uncertainty. In [7-9], such an observation is termed as possible opportunity or windfall brought about by uncertainty. In Figure 1, it is shown that at $x=5.0$, it is possible to obtain a better performance when x deviates to 4.0 on account of the uncertainty. The same can be explained for $x=7.3$, which can even reach the global optimum at $x=7.0$. In this paper we will consider the benefits of uncertainty in our SMIRE algorithm in section 3.2.

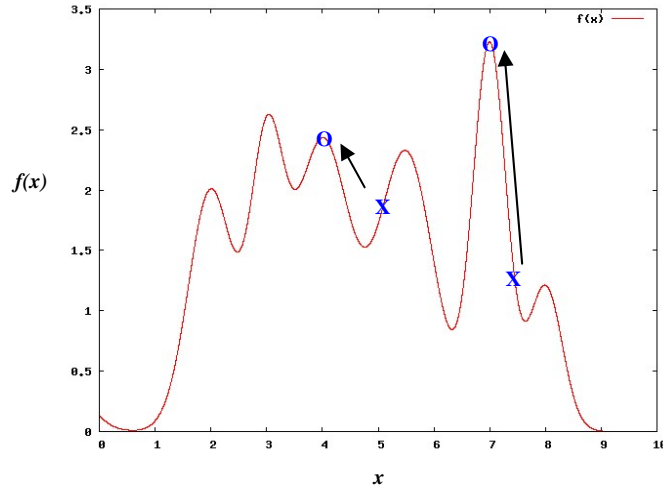


Figure 1. Benefits of uncertainty.

3 Single/Multi-objective Inverse Robust Evolutionary (SMIRE) Design Optimization

In this section, we present the Single/Multi-objective Inverse Robust Evolutionary algorithm for design optimization. In particular, four inverse optimization schemes are introduced.

3.1 Single and Bi-objective SMIRE Design Optimization

Here, we present a scheme for single and bi-objective inverse robust evolutionary design in the presence of uncertainty. The basic steps of the proposed algorithm are outlined in Figure 2. In the first step, the worst-case performance permissible for the final design f_t , and step size Δ used to conduct nested searches are defined and initialised by the designers. The robustness fitness $R_f(x)$ is then defined as the maximum uncertainty a design variable x can handle before violation of f_t . Hence, a design with a larger $R_f(x)$ represents one that is more robust to uncertainty.

Subsequently, a population of designs is created randomly or using Design of Experiments (DOE) techniques such as Latin hypercube sampling or minimum discrepancy sequences [21]. Each individual in the population is evaluated to determine its nominal fitness $f(x)$ and undergoes a sequence of nested searches across a family of nested search regions parameterized by the uncertainty. The aim of the nested searches is to determine the maximum amount of uncertainty that a design solution guarantees to handle before violating the worst-case fitness permissible as defined by f_t .

BEGIN SMIRE (Consider a maximization problem)

Initialization Phase:

- Initialize worst-case permissible performance, f_t
- Initialize the step size Δ for the inner search
- Generate a population of design vectors

Search Phase:

While (termination condition is not satisfied)

For (each individual i in the population)

- Objective-1: $Obj-1 = f(x_i)$, applicable for bi-objective SMIRE
- Objective-2:

○ Assign $k=0$

○ **Repeat**

◇ $k=k+1$

◇ **Minimize:** $f^k(x)$

subject to: $x_l^k \leq x \leq x_u^k$, where $x_l^k = x_i - k\Delta$, $x_u^k = x_i + k\Delta$

◇ Obtain x_{opt}^k and $f(x_{opt}^k)$

◇ Store $f(x_{opt}^k)$ and associate it with $k\Delta$ in database D_b

until $f(x_{opt}^k) \leq f_t$

○ Estimate maximum uncertainty δ_{max}^i by interpolating from $f(x_{opt}^k)$ and $k\Delta$ in D_b

○ $Obj-2 = R_f(x_i) = \delta_{max}^i$

end For

- Apply MOEA (if multi-objective), or EA (if single objective) evolutionary operators to create a new population.

end While

END SMIRE

Figure 2. Single and bi-objective SMIRE design algorithm.

More specifically, for each chromosome, we solve a sequence of bound constrained optimization sub-problems of the form:

$$\begin{aligned} &\mathbf{Minimize} : f^k(x) \\ &\mathbf{Subject to} : x_l^k \leq x \leq x_u^k \end{aligned} \quad (7)$$

where x_l^k and x_u^k are the appropriate bounds on the uncertain parameters. Each k^{th} optimization sub-problem locates the worst-case fitness in the direct neighborhood of individual x within the bounds, x_l^k and x_u^k which are updated with step size Δ :

$$x_l^k = x_i - k\Delta$$

$$x_u^k = x_l + k\Delta \quad (8)$$

In single objective inverse robust evolutionary design optimization, only the robustness function $R_f(x_i)$ is considered. The bi-objective IRE on the hand considers both $R_f(x_i)$ and $f(x)$ is in the design search to locate the pareto-optimum set.

Note that by conducting a sequence of nested searches across a family of ascending nested bounds parameterized by the uncertainty vector, we arrive at a monotonic decreasing function of worst-case fitness versus uncertainty such that:

$$x_l^{k+1} \leq x_l^k, x_u^k \leq x_u^{k+1} \rightarrow f(x_{opt}^k) \leq f(x_{opt}^{k+1}) \quad (9)$$

where x_{opt}^k denotes the optimum at the s iteration and $f(x_{opt}^k)$ is the corresponding worst-case fitness obtained for $x_l^k \leq x \leq x_u^k$. In addition, the $f(x_{opt}^k)$ found and associated $k\Delta$ for each search iteration is then stored to create a database of uncertainties and corresponding worst-case fitness. The sequences of iterative searches are terminated when the optimal solution of the k^{th} sub-problem violates the inequality constraint in eq. (10), i.e.

$$f(x_{opt}^k) \geq f_t \quad (10)$$

At the end of the sequences of searches for a chromosome, the maximum uncertainty δ_{max} that a design may handle given a defined f_t can be determined by interpolating from the database of uncertainties and worst-case fitness values previously archived, i.e., $k\Delta$ and $f(x_{opt}^k)$. The search then proceeds with the standard evolutionary operators to create a new population and stops when the termination conditions are reached. Here, we further illustrate the procedure to locate the robustness fitness using an example in figure 3. Consider the design point at $x=4$ in the figure. Here, f_t and Δ are configured as 4.0 and 1.0, respectively. A sequence of bound-constrained optimization sub-problems are then conducted for $x=4$, which is terminated upon violations of the constraint in eq. (10). The labels A, B and C correspond to $f(x_{opt}^k)$ for $k = 1, 2$ and 3. At $k=3$, the worst-case fitness, indicated by C, has satisfied the termination condition. Then, the estimated maximum amount of uncertainty, δ_{max} the design point $x=4$ can handle is determined by interpolating from A, B, and C.

The computational complexity for establishing the robustness fitness, $R_f(x)$ in SMIRE is of $O(gnkl)$. Here, g is the number of generations for the EA search, n is the number of chromosomes evolved, k is the average number of iterations to reach δ_{max} for each chromosome and l represents the average number of function evaluations incurred in each bound constrained optimization sub-problems. It is worth noting that $k \propto \frac{1}{\Delta}$.

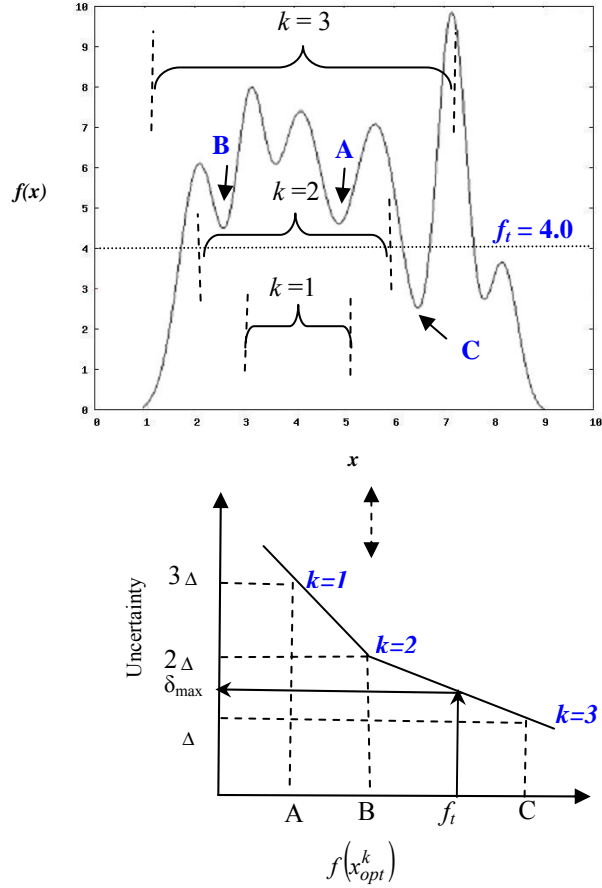


Figure 3. Robustness fitness in SMIRE for $x_t=4.0$ and $\Delta=1.0$

3.2 Tri-objective SMIRE Design Optimization

In this subsection, we proceed from single and bi-objective SMIRE design optimization to consider higher number of objectives. In particular, we search for pareto-optimal solutions when considering nominal, robustness, and opportunity fitness simultaneously. Here we present two tri-objective schemes for exploiting the benefits of uncertainty, i.e. opportunity in the design search.

3.2.1 Three-objective SMIRE Scheme I

A straightforward approach as in [18-20] is to formulate the search problem as a tri-objective scheme which treats all three objectives equally. The procedures to ob-

tain the first two objectives, i.e., nominal $f(x)$ and robustness fitness $R_f(x)$ for each design vector remain the same as described in section 3.1 for the bi-objective IRE. The third objective, i.e. the opportunity fitness, is determined using an approach similar to establishing $R_f(x)$ involving a series of nested optimization search as illustrated in Figure 4.

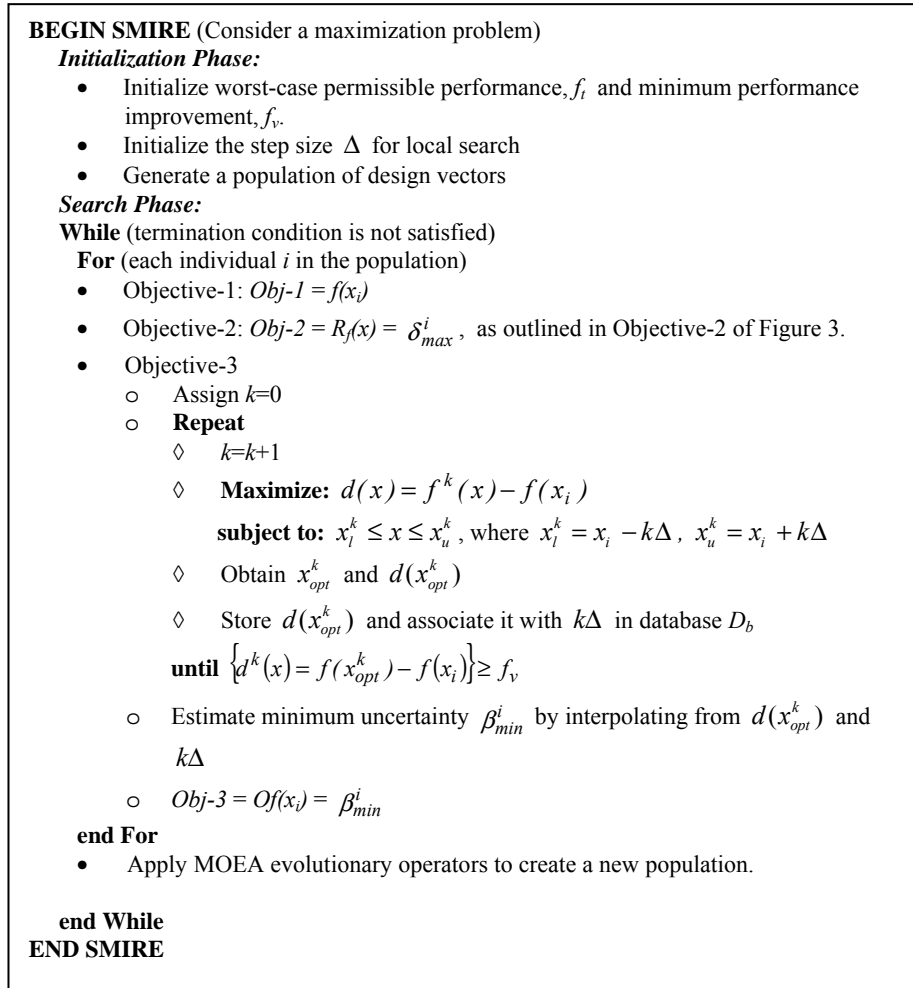


Figure 4. Tri-objective SMIRE design algorithm, scheme I.

The fitness of opportunity function $O_f(x)$ is defined as the minimum uncertainty the design variable x would require in order to acquire a performance improvement defined by f_v . In particular, for each chromosome, we solve a sequence of bound constrained optimization sub-problems in the form:

$$\begin{aligned}
& \textbf{Maximize: } d(x) = f^k(x) - f(x_i) \\
& \textbf{subject to: } x_l^k \leq x \leq x_u^k
\end{aligned} \tag{11}$$

where x_l^k and x_u^k are the appropriate bounds on the uncertain parameters.

Each k^{th} optimization sub-problem locates the best-case fitness in the direct neighborhood of individual x within the bounds, x_l^k and x_u^k which are updated using eq. (8). The search for minimum uncertainty possible at x terminates when the best performance improvement possibly achieved has reached f_v , i.e. $\{d^k(x) = f(x_{opt}^k) - f(x_i)\} \geq f_v$. The minimum uncertainty β_{min}^i is then interpolated from the database of uncertainties and best fitness improvement recorded previously, i.e., $k\Delta$ and $d(x_{opt}^k)$.

The expected computational costs for obtaining $R_f(x)$ and $O_f(x)$ are equivalent. In effect, for the same number of search generations made, the tri-objective IRE scheme is approximately two times more computational expensive than the bi-objective IRE scheme described in section 3.1.

3.2.2 Tri-objective SMIRE Scheme II

Alternatively, one may consider the opportunity function as a secondary objective. In particular, the opportunity fitness is determined only after the robustness fitness is obtained. As a result, the secondary objective is defined as the maximum performance improvement permissible in the presence of uncertainty and given by:

$$\begin{aligned}
& \textbf{Maximize: } Of(x_i) = f(x) - f(x_i) \\
& \textbf{subjected to: } x_i - \delta_{max}^i \leq x \leq x_i + \delta_{max}^i
\end{aligned} \tag{12}$$

where δ_{max}^i is the maximum uncertainty defined by $R_f(x)$. The pseudo-code for scheme II is also outlined in Figure 5.

The computational cost for Tri-objective SMIRE, scheme II may be determined to be of $O(gn(k+1))$. In comparison to other SMIRE schemes introduced earlier, scheme II incurs a higher computational cost than both the single and bi-objective IRE, i.e., $O(gnkl)$, generally lower than the other tri-objective IRE counterpart, i.e., scheme I which is $O(2gnkl)$.

BEGIN SMIRE (Consider a maximization problem)

Initialization Phase:

- Initialize worst-case permissible performance, f_t
- Initialize the step size Δ for local search
- Generate a population of design vectors

Search Phase:

While (termination condition is not satisfied)

For (each individual i in the population)

- Objective-1: $Obj-1 = f(x_i)$
- Objective-2: $Obj-2 = R_f(x) = \delta_{max}^i$, as outlined in Objective-2 of Figure 3.
- Objective-3:
 - **Maximize:** $Of(x_i) = f(x) - f(x_i)$
 - subject to:** $x_i - \delta_{max}^i \leq x \leq x_i + \delta_{max}^i$
 - $Obj-3 = Of(x_i)$

end For

- Apply standard MOEA operators to create a new population.

Figure 5. Tri-objective SMIRE design algorithm, scheme II.

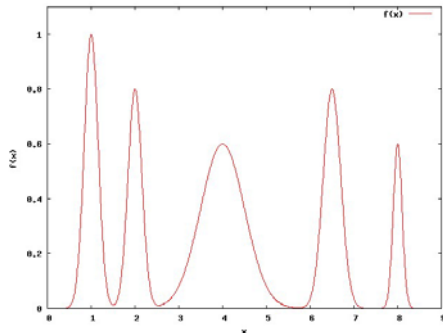
4 Empirical Studies

In this section, we present an empirical study on the proposed SMIRE schemes using five synthetic test functions plotted in Figure 6. These include a three 1D functions (f1, f2 and f3) and two 2D functions (f4 and f5) having the characteristics described in Table 1. It is worth noting that the selection of the low dimensional functions is merely meant for illustration purpose. The methodology can be simply generalized for higher dimensional problems.

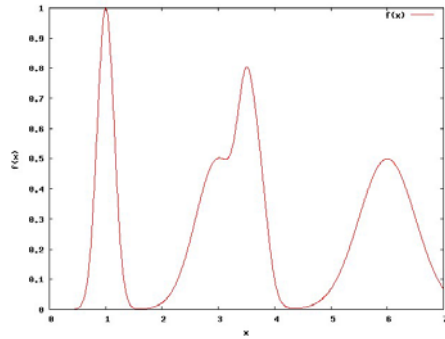
Table 1. Five synthetic test functions were considered in the empirical study.

Test Function	Characteristics of the functions
f1	$f(x) = e^{-(x-1)^2/0.05} + 0.8e^{-(x-2)^2/0.05} + 0.6e^{-(x-4)^2/0.5} + 0.8e^{-(x-6.5)^2/0.08} + 0.6e^{-(x-8)^2/0.02}$ $0 \leq x \leq 9, f_i=0.4 \text{ and } f_v=0.2$
f2	$f(x) = \left(e^{-(x-1)^2/0.5} \right) + 2 \left(e^{-(x-1.25)^2/0.045} \right) + 0.5 \left(e^{-(x-1.5)^2/0.0128} \right) + 2 \left(e^{-(x-1.6)^2/0.005} \right) + 2.5 \left(e^{-(x-1.8)^2/0.02} \right) + 2.5 \left(e^{-(x-2.2)^2/0.02} \right) + 2 \left(e^{-(x-2.4)^2/0.005} \right) + 2 \left(e^{-(x-2.75)^2/0.045} \right) + \left(e^{-(x-3)^2/0.5} \right) + 2 \left(e^{-(x-6)^2/0.32} \right) + 2.2 \left(e^{-(x-7)^2/0.18} \right) + 2.4 \left(e^{-(x-8)^2/0.5} \right) + 2.3 \left(e^{-(x-9.5)^2/0.5} \right) + 3.2 \left(e^{-(x-11)^2/0.18} \right) + 1.2 \left(e^{-(x-12)^2/0.18} \right)$

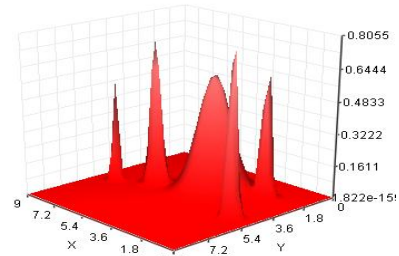
	$-1 \leq x \leq 13, f_t=1.5$ and $f_v=1$
f3	$f(x) = e^{-(x-1)^2/0.045} + \frac{1}{2}e^{-(x-3)^2/0.32} + \frac{1}{2}e^{-(x-3.5)^2/0.045}$ $+ \frac{3}{10}e^{-(x-3.75)^2/0.045} + \frac{1}{2}e^{-(x-6)^2/0.5}$
	$0 \leq x \leq 7, f_t=0.3$ and $f_v=0.2$
f4	$f(x,y) = \left(e^{-[(x-1)^2+(y-5)^2]/0.05} \right) + 0.8 \left(e^{-[(x-2)^2+(y-2)^2]/0.05} \right) +$ $0.6 \left(e^{-[(x-4)^2+(y-3)^2]/0.5} \right) + 0.8 \left(e^{-[(x-6.5)^2+(y-4)^2]/0.08} \right) +$ $0.6 \left(e^{-[(x-8)^2+(y-5)^2]/0.02} \right)$
	$0 \leq x, y \leq 9, f_t=0.4$ and $f_v=0.2$
f5	$f(x,y) = \left(e^{-((x-1)^2+(y-5)^2)/0.5} \right) + 2 \left(e^{-((x-1.25)^2+(y-5)^2)/0.045} \right) +$ $0.5 \left(e^{-((x-1.5)^2+(y-5)^2)/0.0128} \right) + 2 \left(e^{-((x-1.6)^2+(y-5)^2)/0.005} \right) +$ $2.5 \left(e^{-((x-1.8)^2+(y-5)^2)/0.02} \right) + 2.5 \left(e^{-((x-2.2)^2+(y-5)^2)/0.02} \right) +$ $2 \left(e^{-((x-2.4)^2+(y-5)^2)/0.005} \right) + 2 \left(e^{-((x-2.75)^2+(y-5)^2)/0.045} \right) +$ $\left(e^{-((x-3)^2+(y-5)^2)/0.5} \right) + 2 \left(e^{-((x-6)^2+(y-7)^2)/0.32} \right) +$ $2.2 \left(e^{-((x-7)^2+(y-7)^2)/0.18} \right) + 2.4 \left(e^{-((x-8)^2+(y-7)^2)/0.5} \right) +$ $2.3 \left(e^{-((x-9.5)^2+(y-7)^2)/0.5} \right) + 3.2 \left(e^{-((x-11)^2+(y-7)^2)/0.18} \right) +$ $1.2 \left(e^{-((x-12)^2+(y-7)^2)/0.18} \right)$
	$-1 \leq x, y \leq 13, f_t=1.5$ and $f_v=1$



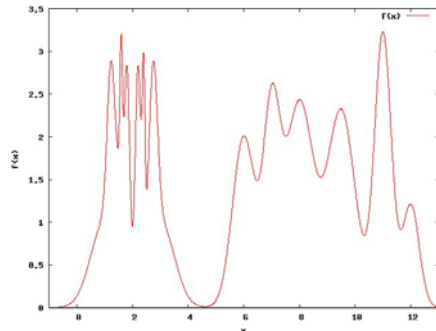
(a) f1



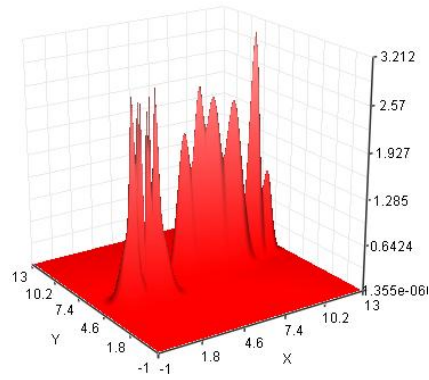
(c) f_3



(d) f_4



(b) f_2



(e) f_5

Figure 6. 2D and 3D plots of the test functions considered

In the numerical studies, we employ a 16-bit binary coded standard GA for single objective SMIRE and NSGA [17] for multi-objective SMIRE. A linear ranking algo-

rithm is used for selection in the standard GA. The population size is kept at 100, and maximum generation count is set to 100 generations. Uniform crossover and mutation are applied at probabilities of 0.9 and 0.01, respectively. The step size Δ is chosen empirically to be 3% from the range of search space, which is considered sufficient to minimize interpolation error. In the nested optimizations, a local search based on Feasible Sequential Quadratic Programming (FSQP) is utilized.

4.1 Discussions on Different SMIRE Schemes

Figure 7 and 8 show the different pareto-optimum solution sets in the parameter space, obtained when using the four SMIRE schemes on f1 and f2 respectively.

When the single objective IRE is applied, it is as expected that the final global optimum solution will lie on the most robust peak, which is generally the highest point in the widest peak and having nominal fitness greater than f_i . For instance, the most robust point is approximately at $x = 4.0$ for f1 and $x = 8.0$ for f2. Then, using the bi-objective IRE, the solution set now comprised of those with trade-off between the two objectives considered in the scheme. It is worth noting that in a low-multimodal function such as f1, the solution for the bi-objective scheme simply consists of one with best nominal and one with best robustness, which are located at different peaks in this test function. However, in high-multimodal function such as f2, it is generally the case that more trade-offs between the nominal and robustness fitness, hence more different solutions in the pareto-optimum solution set. Employing the tri-objective schemes, the solution set now is even more varied as more trade-offs between nominal, robustness, and opportunity fitness are expected. The difference between the solutions from tri-objective scheme I and II will be discussed further in next subsection.

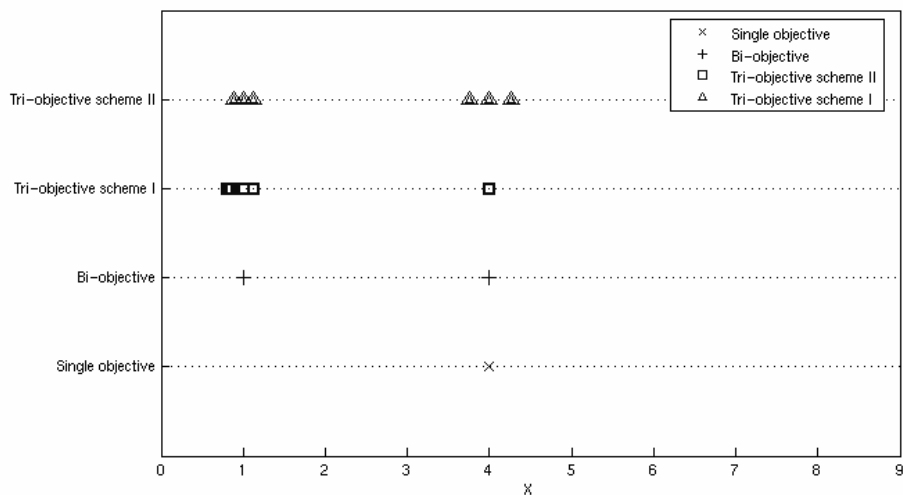


Figure 7. Pareto-optimum solutions of SMIRE on f1.

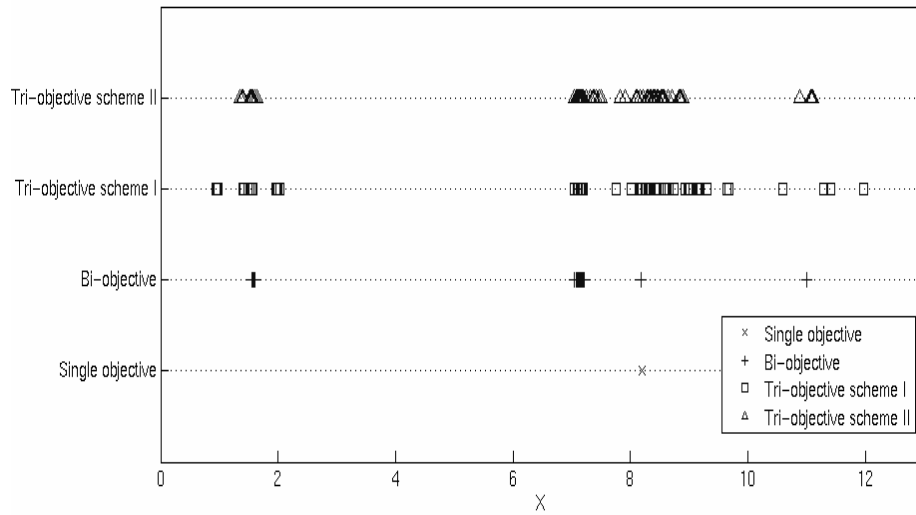


Figure 8. Pareto-optimum solutions of SMIRE on f_2 .

4.2 Comparison on Tri-objective IRE Scheme I and II

To better illustrate the difference on tri-objective IRE scheme I and II, we study the pareto-optimum solutions obtained in f_3 , f_4 , and f_5 at their parameter space. For f_3 , the pareto-optimum solutions obtained for both schemes are presented in Figure 9 and 10.

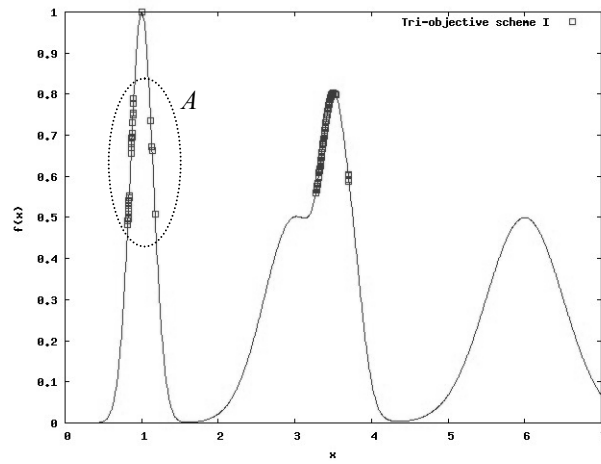


Figure 9. Pareto-optimum solutions of tri-objective IRE scheme I on f_3 .

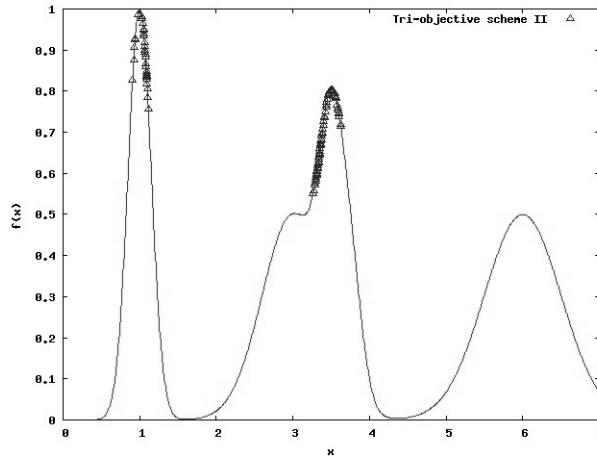


Figure 10. Pareto-optimum solutions of tri-objective IRE scheme II on f_3 .

In the first scheme as in Figure 9, the opportunity fitness is treated equally to other robustness and nominal fitness, hence there might be solutions exist just because of its good opportunity fitness even though poor in other objectives. This type of solutions, usually exist in a steep peak, e.g. the solutions indicated by label A in the figure. In contrast, the second scheme (see Figure 10) requires a solution to be robust before the opportunity fitness is considered. Hence, we might expect that solutions with good opportunity fitness in the first scheme might not appear in the second scheme, especially those located at a steep and not-robust peaks. As the result of the tri-objective scheme II, the solutions on the robust peaks have better opportunity to acquire benefits from uncertainty. This fact is again shown in the pareto-optimum solutions for 2D functions, f_4 and f_5 as presented in Figure 11, 12, 13, and 14. Figure 11 and 13 demonstrate that applying tri-objective scheme I, there might be many of the pareto-optimum solutions exist near the steep peaks, without considering their robustness. Conversely, Figure 12 and 14 clearly exhibit the characteristic of tri-objective scheme II which treat the opportunity fitness as secondary objective, hence most of the solutions still lie on the robust peaks.

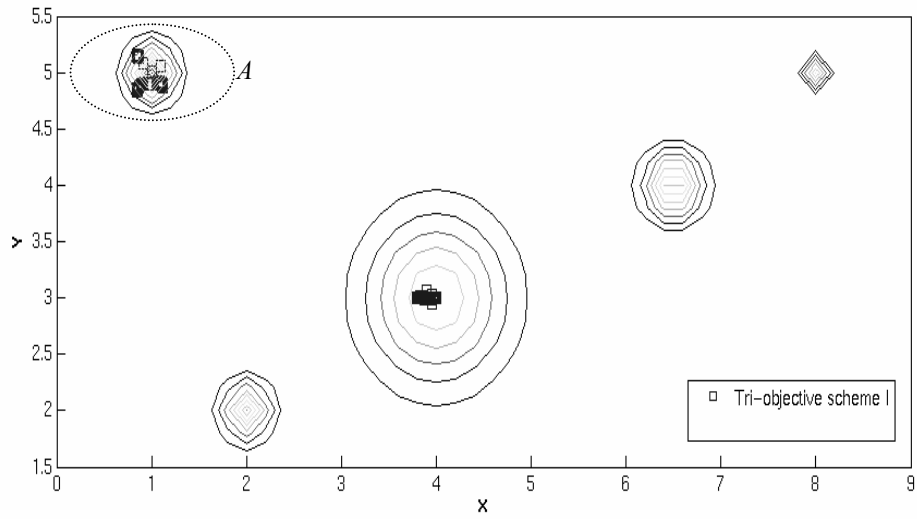


Figure 11. Pareto-optimum solutions of tri-objective IRE scheme I on f4.

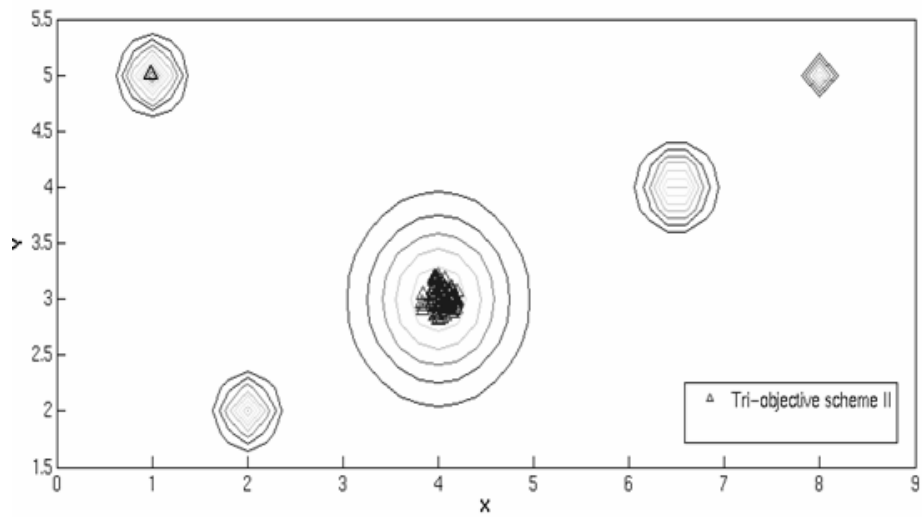


Figure 12. Pareto-optimum solutions of tri-objective IRE scheme II on f4.

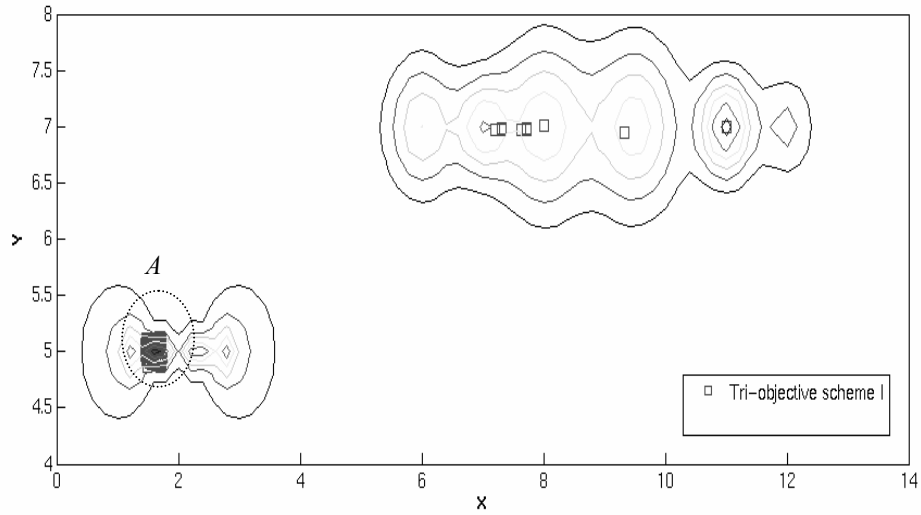


Figure 13. Pareto-optimum solutions of tri-objective IRE scheme I on f5.

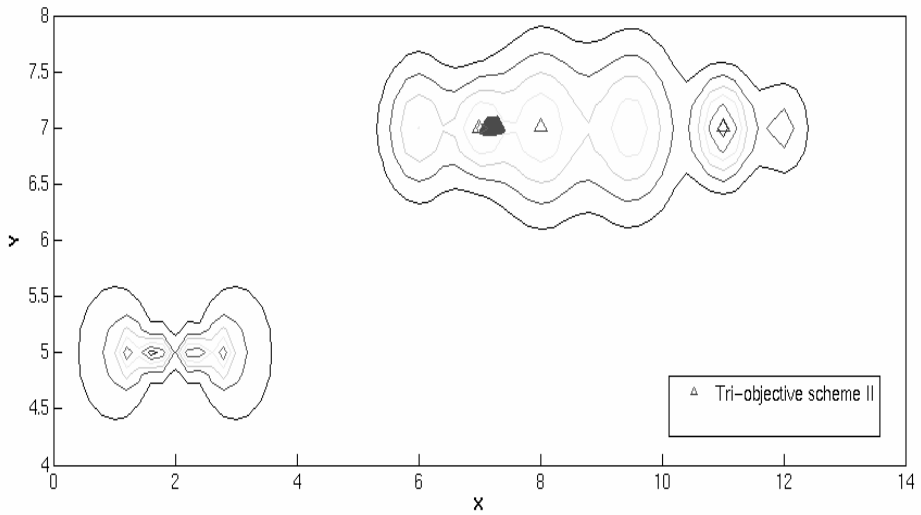


Figure 14. Pareto-optimum solutions of tri-objective IRE scheme II on f5.

Another important point to note in the application of the tri-objective IRE schemes is the computational cost incurred. This is shown in Table 2 which lists the comparison of the computational cost between the two schemes in terms of objective function evaluations incurred for the five test functions. It is generally the case that scheme I requires greater computational cost compared to scheme II.

Table 2. Ratio of computational cost incurred in IRE scheme I and II.

Test Function	Ratio of Computational Cost between Tri-objective Scheme I and II
f1	1:0.78
f2	1:0.66
f3	1:0.75
f4	1:0.81
f5	1:0.62

5 Conclusion

In this paper, we have presented the single and multi-objective inverse robust evolutionary design optimization in the presence of uncertainty. It proposes the use of inverse optimization technique in the field of robust optimization. Another important feature of the proposed methodology is that the solutions obtained were discovered without any requirement to make possible untrue assumptions about the structure of the uncertainties involved as what usually available in probabilistic methods. In addition, we have also presented the incorporation of the opportunity fitness to possibly explore the benefit of having uncertainty in design. Hence, the final solutions obtained provide the decision-makers or designers with more design options considering the trade-offs up to three objectives: robustness, nominal fitness, and opportunity fitness.

In evolutionary algorithms, many thousands of calls to the objective function are often required to locate a near optimal solution. While the algorithm proposed offers an effective approach to modeling of uncertainty in engineering design, a compelling limitation of the theory is the massive computational efforts incurred in the nested evolutionary design search. A simple solution to this issue would be to replace the nested global optimization with local search which is much cheaper as demonstrated in [16]. The computational efforts incurred would be even more devastating if the objective function is computationally expensive which is very common in complex engineering design problems. Nevertheless, it is worth noting here that a promising and intuitive way to reduce the search time incurred in solving the sequences of bound constrained sub-problems is to replace as much as possible the computationally expensive high-fidelity analysis solvers with lower-fidelity models that are computationally less expensive. The readers are referred to [22-24] for greater details on the algorithm available to achieve this cost savings.

Acknowledgement

The authors would like to thank the Parallel and Distributed Computing Centre at the School of Computer Engineering, Nanyang Technological University for providing support and computing resources to this work.

References

- [1] Goldberg D.E., "Genetic Algorithms in Search, Optimization and Machine Learning", 1989.
- [2] Jin Y., Branke J., "Evolutionary Optimization in Uncertain Environment-A Survey", *IEEE Transactions on Evolutionary Computation*, Vol. 9, No. 3, June 2005.
- [3] Ong Y.S., Nair P.B., Lum K.Y., "Min-Max Surrogate Assisted Evolutionary Algorithm for Robust Aerodynamic Design", *Special Issue on Evolutionary Optimization in the Presence of Uncertainties*, IEEE Transactions on Evolutionary Computation, Accepted, 2005.
- [4] Oberkampf, W. L., et al., "Estimation of Total Uncertainty in Modeling and Simulation," *Sandia Report SAND2000-0824*, 2000.
- [5] Oberkampf, W., Helton, J., Sentz, K., "Mathematical Representation of Uncertainty," *AIAA Proceedings of Non-Deterministic Approaches Forum*, Reston, VA, 2001.
- [6] Ben-Haim Y., "Information Gap Decision Theory", California: Academic Press, 2001.
- [7] Ben-Haim Y., "Uncertainty, Probability, and Information-Gaps", *Reliability Engineering and System Safety* 85, pp. 249-266, 2004.
- [8] Ben-Haim Y., "Robust Reliability in Mechanical Sciences", Springer-Verlag, Berlin, 1996.
- [9] L. Huyse, "Solving Problems of Optimisation Under Uncertainty as Statistical Decision Problems", *AIAA-2002-1519*, 2001.
- [10] Tsutsui S. and Ghosh A., "Genetic Algorithms with a Robust Solution Searching Scheme", *IEEE Transaction on Evolutionary Computation*, Vol. 1, No. 3, pp. 201-208, 1997.
- [11] Arnold D. V. and Beyer H. G., "Local Performance of the (1+1)-ES in a Noisy Environment", *IEEE Trans. Evolutionary Computation*, Vol. 6, No. 1, pp 30-41, 2002.
- [12] Huyse L. and Lewis R.M., "Aerodynamic Shape Optimization of Two-dimensional Airfoils Under Uncertain Operating Conditions", Hampton, Virginia: ICASE NASA Langley Research Centre, 2001.
- [13] Anthony D.K. and Keane A.J., "Robust Optimal Design of a Lightweight Space Structure Using a Genetic Algorithm", *AIAA Journal* 41(8), pp. 1601-1604, 2003.
- [14] Wiesmann D., Hammel U. and Back T., "Robust design of multilayer optical coatings by means of evolutionary algorithms", *IEEE Trans Evolutionary Computation*, Vol 2, No 4, pp 162-167, 1998.
- [15] Markovitz, H.M., "Portfolio Selection," *J. Finance*, Vol. 7, pp. 77-91, 1952.
- [16] Lim D., Ong Y.S., Lee B.S., "Inverse Multi-Objective Robust Evolutionary Design Optimization in The Presence of Uncertainty", *Workshop on Evolutionary Algorithm for Dynamic Optimization Problems, Genetic and Evolutionary Computation Conference (GECCO)*, Washington, 2005.
- [17] Srinivas N. and Deb K., "Multiobjective Optimization Using Nondominated Sorting in Genetic Algorithms," *Evolutionary Computation*, 2(3):221-248, 1994.
- [18] Ray. T., "Constrained Robust Optimal Design Using a Multiobjective Evolutionary Algorithm", *Proceedings of Congress on Evolutionary Computation*, 2002.
- [19] Jin Y. and Sendhoff B., "Trade-Off between Performance and Robustness: An Evolutionary Multiobjective Approach", *Proceedings of Second International Conference on Evolutionary Multi-criteria Optimization*. LNCS 2632, Springer, pp.237-251, Faro, 2003.
- [20] Li M., Azarm S., Aute V., "A Multi-Objective Genetic Algorithm for Robust Design Optimization", *Genetic and Evolutionary Computation Conference (GECCO)*, Washington, 2005.
- [21] Fang K.T., Ma C.X., and Winker P., "Centered L2-Discrepancy of Random Sampling and Latin Hypercube Design, and Construction of Uniform Designs", *Mathematics of Computation*, Vol. 71, No. 237, pp. 275-296, 2000.

- [22] Jin Y. and Sendhoff B., "Fitness approximation in evolutionary computation: A survey", *Proceedings of the Genetic and Evolutionary Computation Conference*, pages 1105-1112, 2002.
- [23] Ong Y.S., Nair P.B. and Keane A.J., "Evolutionary Optimization of Computationally Expensive Problems via Surrogate Modeling", *AIAA Journal*, Vol. 41, No. 4, pp 687-696, 2003.
- [24] Ong Y.S., Lum K.Y., Nair P.B., Shi D.M. and Zhang Z.K., "Global Convergence of Unconstrained and Bound Constrained Surrogate-Assisted Evolutionary Search in Aerodynamic Shape Design Solvers", *IEEE Congress on Evolutionary Computation*, Special Session on Design Optimization with Evolutionary Computation", 2003.